



3D Material Characterization and Determination of Out-Of-Plane Properties Based on Digital Image Correlation

Nikolas Korte¹(✉), Jens Bold², Alexander Hüls³, Sascha Ort³,
Bernd Westerhoff³, Bruno Musil¹, and Philipp Höfer¹

¹ Universität Der Bundeswehr München, 85577 Neubiberg, Germany
{nikolas.korte,bruno.musil,philipp.hoefer}@unibw.de

² Boeing Deutschland GmbH, 80805 Munich, Germany
jens.bold@boeing.com

³ VORWERK AUTOTEC GmbH & Co. KG, 42287 Wuppertal, Germany
{a.huels,s.ort,b.westerhoff}@vorwerk-automotive.de

Abstract. In this work, an approach for a 3D material characterization based on experiments is presented. Experimentally determined material properties are used to define a 3D compliance matrix for a more accurate simulation of the material's behavior. This includes out-of-plane properties, e.g. transverse contraction in thickness direction. To gain complete stress-strain curves in material testing, Digital Image Correlation (DIC) is used for strain measurement. Through the usage of a biplane DIC-setup, out-of-plane measurements including strains in thickness direction are possible. Unidirectional endless fiber composites and short fiber plastic were tested in tension and compression to determine in-plane and out-of-plane material properties, each for two material orientations.

Simulations of the short fiber plastic injection molding process lead to fiber orientations over the thickness, which are compared to computer tomographic (CT) scans. With adjusted distribution of fiber orientations, simulations of mechanical behavior in all three directions are presented and compared to test data.

Keywords: 3D Material Characterization · Digital Image Correlation · Out-of-plane Properties · Strains in Thickness Direction · Composites · CFRP · Short Fiber Plastic

1 Introduction

Composite parts have a high potential in weight saving for aerospace as well as automotive applications. In order to exploit this potential, a precise knowledge of the material's behavior is necessary. For a complete description of the material behavior, various material properties must be determined experimentally in different material directions and under different test methods. Some of these materials values, like

out-of-plane properties, are often only assessed based on literature or very thick laminates. For orthotropic materials, strains can be correlated with the stress vector and a 3D compliance matrix within a linear-elastic region, see Eq. 1 [1]. Here, the compliance matrix contains 12 engineering constants, that must be determined in experiments.

$$\begin{pmatrix} \varepsilon_1 \\ \varepsilon_2 \\ \varepsilon_3 \\ \gamma_{23} \\ \gamma_{31} \\ \gamma_{12} \end{pmatrix} = \begin{bmatrix} \frac{1}{E_1} & -\frac{\nu_{21}}{E_2} & -\frac{\nu_{31}}{E_3} & & & \\ -\frac{\nu_{12}}{E_1} & \frac{1}{E_2} & -\frac{\nu_{32}}{E_3} & & & \\ -\frac{\nu_{13}}{E_1} & -\frac{\nu_{23}}{E_2} & \frac{1}{E_3} & & & \\ & & & \frac{1}{G_{23}} & & \\ & & & & \frac{1}{G_{31}} & \\ & & & & & \frac{1}{G_{12}} \end{bmatrix} \begin{pmatrix} \sigma_1 \\ \sigma_2 \\ \sigma_3 \\ \tau_{23} \\ \tau_{31} \\ \tau_{12} \end{pmatrix} \quad (1)$$

For in-plane properties (1- and 2-direction), standard tests are well established for orthotropic materials like unidirectional or woven endless fiber reinforced plastics, shown in Fig. 1.

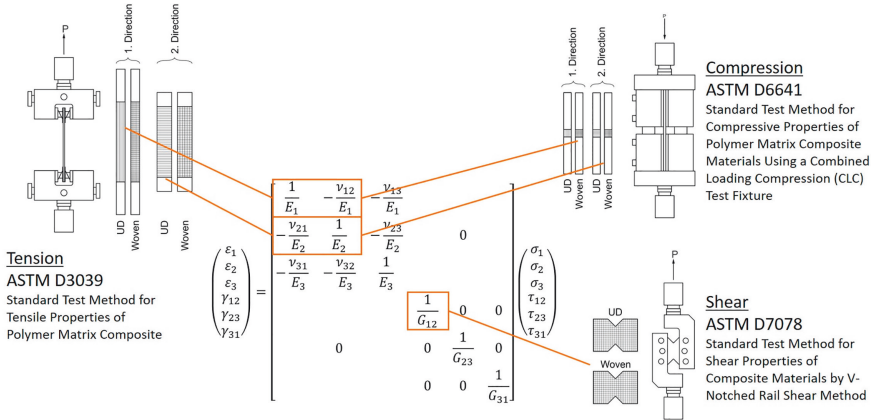


Fig. 1. 3D compliance matrix of polymer matrix composite including standard test methods for each material property

If a unidirectional laminate is regarded as a layup of individual plies in which the fibers with constant cross-section are arranged exactly parallel and have a uniform packing density, it is referred to as an ideal ply. This idealization also includes complete fiber-matrix adhesion, as well as the absence of pores, etc. [2].

For such ideal layers of unidirectional laminates, it is then considered to have transversal isotropic properties due to the same fiber architecture in 2- and 3-direction. This idealization leads to a reduction of the orthotropic compliance matrix in Eq. 1, where $E_3 = E_2$, $\nu_{31} = \nu_{21}$ and $G_{13} = G_{12}$ [1, 2].

For short fiber reinforced plastic, where the direction of the fiber is changing through the thickness, necessary values and allowable cannot be directly determined from standard tests because not a single direction like in the coupon test for endless fibers is tested. This corresponds to element tests for endless fibers. Additionally, for all types of fibers, the values and allowable related to the third direction are generally not measured in standard testing.

Standard tests, based on flat specimens in tension and compression were investigated with the use of 3D Digital Image Correlation (DIC) strain measurement. The 3D DIC not only offers complete stress-strain curves [3] which is necessary to use advanced failure criteria and material models in simulation. Beside strain values in in-plane, the authors present strain measurements in the out-of-plane (thickness) direction. With these test data, it is now possible to determine Poisson's ratios for different directions (ν_{12} , ν_{13} , ν_{21} , ν_{23}) and to compare dependencies of the material direction. In this work, different materials were investigated: short glass-fiber reinforced polyamide 6 and unidirectional carbon fiber laminate.

Simulations with standard and extended material values were performed for the short fiber plastic and compared to the experiments.

2 Experimental Work

2.1 Strain Measurement Using Digital Image Correlation

In this work, strain measurement is performed by Digital Image Correlation (DIC). To gain thickness information during testing, e.g. strains in thickness direction, a biplane DIC-Setup is used. Therefore, the two surfaces of each specimen are observed with two or three cameras, so that both surfaces can be mapped in 3D using the DIC-software (ISTRA 4D, Dantec Dynamics). Figure 2 shows a schematic illustration of the DIC-Setup. All specimens are prepared with a random speckle-pattern for a grey-value estimation performed by the DIC-Software. Each surface is separated into several facets for which displacement und strain values are calculated. Generally, the distance of these two surfaces represents the specimen's thickness. In-plane strains are calculated by the facet's deformation, while out-of-plane strains are calculated by the relative distance change of two facets, lying oppositely on the two mapped specimen surfaces. In this work, all calculated strains are mean values of several facets in a rectangular evaluation field of about 5×3 mm (length x width), depending on the specimens.

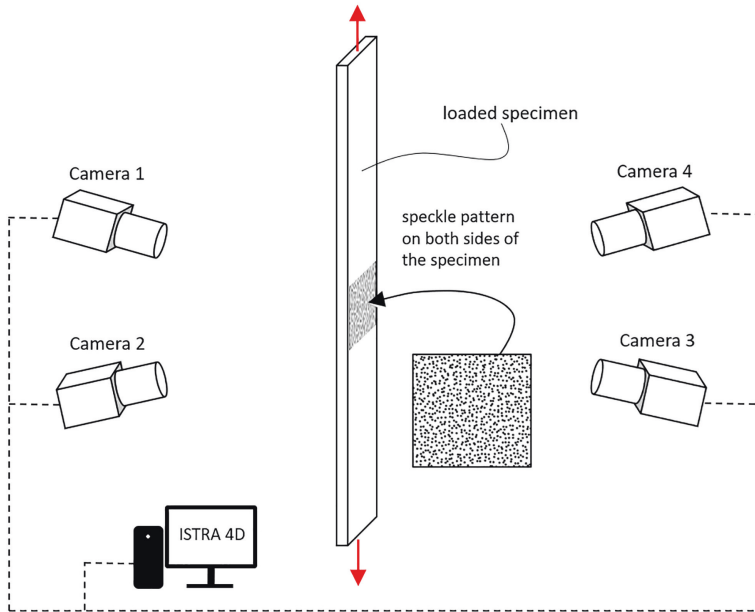


Fig. 2. Schematic illustration of a biplane DIC-Setup

2.2 Specimens and Test Device

An overview of tested materials, specimens and test methods in this work is shown in Table 1. All tests were driven on a Zwick Z150 testing machine with a speed of 1 mm/min.







Table 1. Overview of tested specimens

Material	Test method	Standard (acc. to)	Dimensions [mm]	Thickness [mm]	Number of specimens	Fixture / Grip
CFRP UD-Plain	Tensile 0°	ASTM D3039	250 × 15	2	5	Hydraulic grip
	Tensile 90°		225 × 25	2	5	Hydraulic grip
	Compression 0° and 90°	ASTM D6641	140 × 13	2	4 and 4	Hydraulic Composites Compression Fixture
Short Fiber Plastic	Tensile in- and crossflow		Dogbone 140 × 6	3	3 and 3	Wedge screw grip
	Compression in- and crossflow		Dogbone 140 × 6	3	7 and 8	Hydraulic Composites Compression Fixture

Unidirectional Carbon Fiber Plastic (CFRP-UD). Specimens were cut with the use of a diamond saw or milled out of a plate using diamond coated milling tools. According to ASTM D3039 and ASTM D6641, the specimen's dimensions were 250×15 mm in 0° fiber direction (tensile) and 225×25 mm in 90° fiber direction (tensile) with a free length of 125 mm, as well as 140×13 mm in 0° and 90° fiber direction (compression) [4, 5].

Short Fiber Plastic. Plates of 3 mm thickness were mold-injected with short glass fibers and polyamide 6 matrix. After injection, specimens were milled in inflow and crossflow direction, using the same dogbone geometry for tension and compression testing. Before testing and application of the speckle pattern, the specimens are dried in an oven at slightly elevated temperature for several days until relative weight loss is nearly asymptotic.

Table 2. Tested specimens

Test method	Specimen
Tensile CFRP UD 0°	
Tensile CFRP UD 90°	
Compression CFRP UD 0°	
Compression CFRP UD 90°	
Tensile Short Fiber Plastic	
Compression Short Fiber Plastic	

2.3 Test Results

In the following stress-strain diagrams, the colors of the single curves are according to the shown cartesian coordinate system, where the x-direction corresponds to the loading direction, whereas the y-direction is orthogonally on the specimen's surface. The z-direction is directed towards the thickness and out-of-plane direction.

Due to high noise in the DIC calculated strains in z-direction, this data is filtered by a moving average over nine data points, which was sufficient for an average curve. By the use of an additional camera aligned on the specimen's side to perform an additional 2D-DIC measurement, the measurement noise in z-strains is lower compared to the calculation through the relative thickness change of the two mapped surfaces. Therefore, no additional moving average was performed here. This setup was used only in one test series (tensile CFRP UD 90°). Material properties are calculated using linear regression between datapoints of $\varepsilon_{x,1} = 1000 \frac{\mu m}{m}$ and $\varepsilon_{x,2} = 3000 \frac{\mu m}{m}$ of strain in load direction. For every material and both orientations (0° and 90° , or inflow and crossflow) mean values and their standard deviation are presented. Material properties

were calculated as follows, using a linear regression approach for loading in 1-direction (CFRP UD 0° or short fiber plastic inflow):

$$\nu_{12} = -\frac{\Delta\varepsilon_y}{\Delta\varepsilon_x} \quad (2)$$

$$\nu_{13} = -\frac{\Delta\varepsilon_z}{\Delta\varepsilon_x} \quad (3)$$

The Poisson's ratios ν_{21} and ν_{23} represent the transverse contraction of the material loaded in 90° or crossflow direction with the same quotient of local strain differences. In this work, applied tensile forces result in positive stresses and positive strains in axial direction, whereas applied compressive forces are defined as negative resulting stresses and strains in axial direction.

Tensile CFRP UD 0° and 90° . Stress-strains curves of the tensile tested CFRP specimens are shown below. In Fig. 3a, strains in x-direction (red curves) show a clear, nearly linear curve for the 0° specimens. On the other hand, z-strains (blue curves) show a high noise in the data, which was filtered as described above. Some specimens show positive z-strains at the beginning of the test, whose possible cause has to be further investigated (e.g. uncertainties in DIC z-strain calculation, gripping-effects or other). Fig. 3b shows the stress-strain curves of 90° tensile testing, where an additional camera was faced towards the small specimen's plane. Hereby, an additional 2D-DIC measurement was done, which shows less measurement noise of z-strains. An offset of the single curves of the z-strains can be observed, which again has to be investigated in the near future.

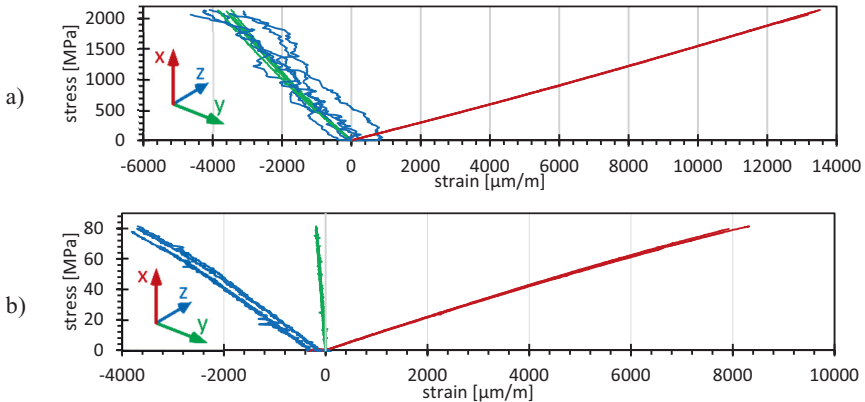


Fig. 3. Stress-strain curves of CFRP UD **a** 0° and **b** 90° tensile testing

Compression CFRP UD 0° and 90° . Strains in x-direction of compression tests are shown as an average of front- and backside at each timestep of each specimen in Fig. 4a for 0° and b for 90° specimens. Again, strains in z-direction of the 0° specimens show an elevated noise in the measurements. The noise of strains in z-direction

in Fig. 4b seems to be lower, but due to the high strain values until rupture, the noise is only poorly visible in this diagram.

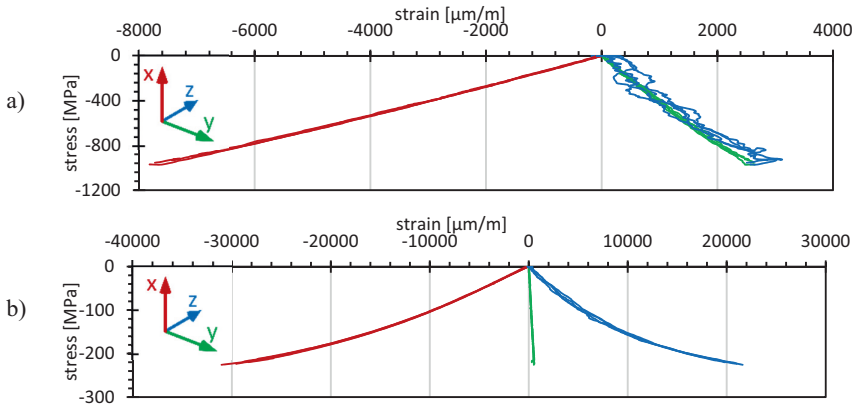


Fig. 4. Stress-strain curves of CFRP UD **a** 0° and **b** 90° compression testing

Determined Material Properties of CFRP UD 0° and 90°. In Fig. 5, the determined material properties based on the previously presented test data is shown. Figure 5a shows material properties for the 0° tensile and compression specimens, Fig. 5b for the 90° tensile and compression specimens. Comparing one material direction for different load direction (tension and compression), stiffness and Poisson’s ratios are different. Major differences in stiffness and transverse contraction, e.g. E_1 and E_2 , or ν_{12} and ν_{21} are based on the unidirectional carbon fiber lying either in load direction or orthogonally to it.

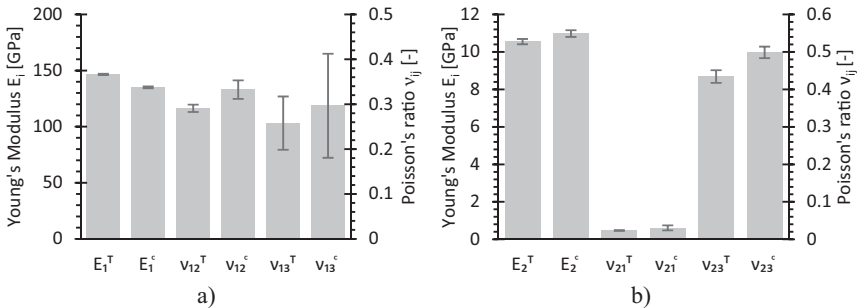


Fig. 5. Determined tension and compression material properties of CFRP UD **a** 0° and **b** 90°

Calculated values for Poisson’s ratios including the third direction show partly high standard deviations due to measurement noise in the calculated z-strains.

Nevertheless, differences between ν_{13} and ν_{23} are observed, which may indicate, that these material properties depend on the load direction for this material. Also, these values are different from values of in-plane transverse contraction ν_{12} and ν_{21} .

Tensile Short Fiber Plastic Inflow and Crossflow. Test data of the second material tested is shown in the next diagrams. Again, two directions of the material are con-sidered. In Fig. 6, tensile test data of a) inflow and b) crossflow direction of the short fiber plastic is presented. Ultimate strains in load direction (x) for the inflow direction specimens are lower but ultimate stresses are higher compared to crossflow direction specimens. In both diagrams, it is clearly shown that strains in y- and z-direction differ from each other.

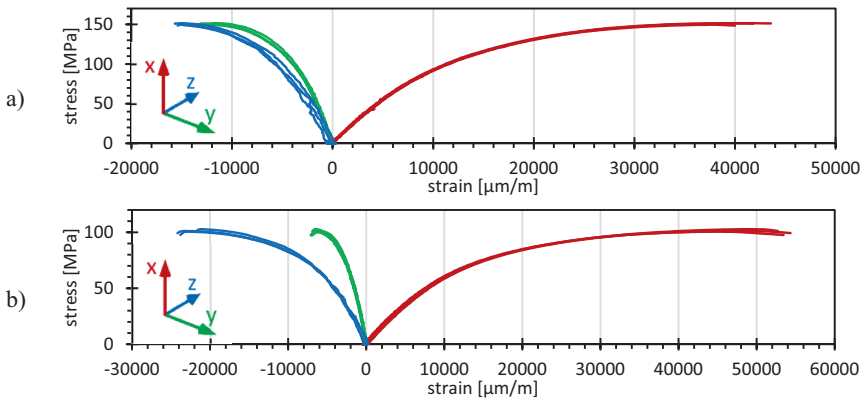


Fig. 6. Stress-strain curves of short fiber plastic **a** inflow and **b** crossflow tensile testing

Compression Short Fiber Plastic Inflow and Crossflow. In compression tests, strain in load direction (x) is averaged from the front- and backside of the specimen.

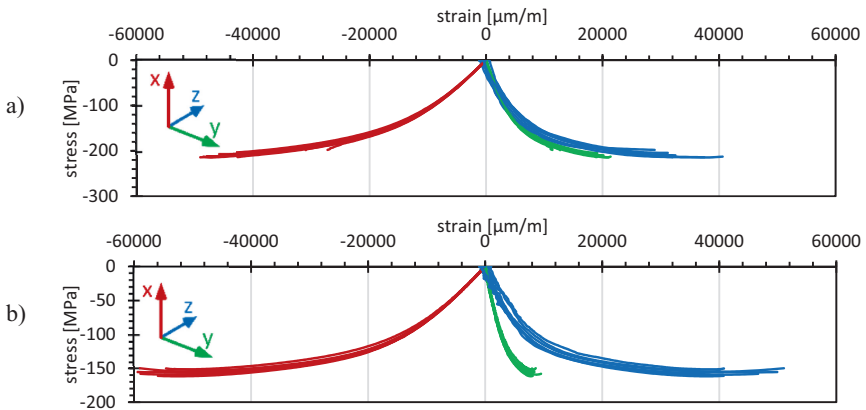


Fig. 7. Stress-strain curves of short fiber plastic **a** inflow and **b** crossflow compression testing

Qualitatively, differences of ultimate strains and stresses in the single directions are similar to tension tests.

Determined Material Properties of Short Fiber Plastic Inflow and Crossflow.

With the data of tension and compression tests shown above, material properties were calculated. Figure 8a shows material properties for the inflow specimens, Fig. 8b for the crossflow specimens. For both material orientations, compression stiffness is higher than tension stiffness. Due to the expected different fiber orientations of the materials, stiffness values are different comparing the material orientation. Here the inflow specimens show a higher Young's modulus.

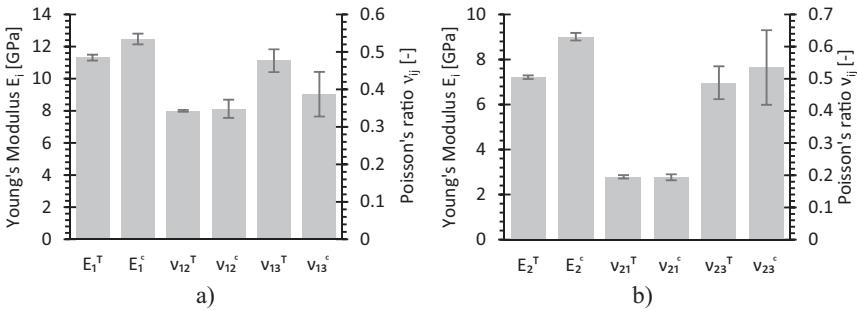


Fig. 8. Determined tension and compression material properties of short fiber plastic

Also, the Poisson's ratio ν_{12} shows higher values than ν_{21} for the crossflow specimens indicating the higher degree of fiber orientation in inflow direction. Standard deviations in Poisson's ratio containing the third direction (ν_{13} , ν_{23}) are elevated again, probably due to higher measurement noise in z-strains.

3 Simulation

3.1 Injection Molding Simulation

In order to capture the fiber orientations of the short fiber plastic, the manufacturing process of plates were simulated. The plate geometry was simulated by means of the filling simulation software CadMould. The plates of thickness 3 mm are the basic material for the later milled testing samples. With the target of getting a realistic output, the relevant areas including the thermal system of the injection tool were replicated. Other parameters of the simulation have been chosen according to measured data of the real process. The fiber orientation result is decomposed into layers along the thickness direction. Due to symmetry, only one half of the thickness is regarded. Here, layer 1 corresponds to the inside layer starting from the symmetry plane and layer 5 to the outside layer of the plate (see Fig. 9).

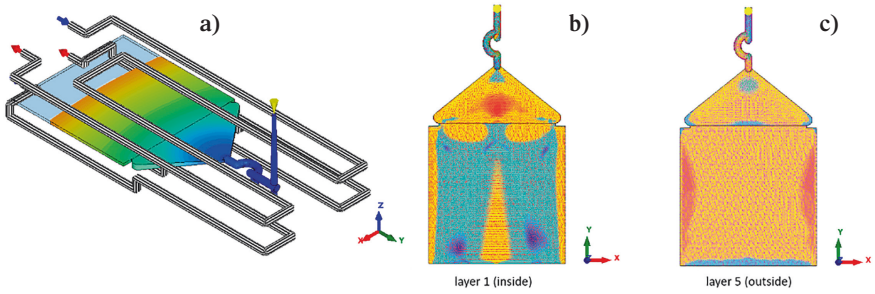


Fig. 9. Fill simulation: **a** layout, **b** layer 1 (*inside*) and **c** layer 5 (*outside*)

In-between there are further 3 layers as results available. Furthermore, the orientations are determined in two directions across the cross section as inflow and crossflow (see Fig. 10). Due to 2.5D fill simulation method the third direction is only a constant value. The fiber orientation of the plate model was then exported as a relevant result for further investigations.

Based on this software export, the fiber orientations were investigated layer-wise along the plate thickness and compared with measurements of the manufactured plates using CT scans. The simulation results of the fiber orientations are partly different from the measured values (see Fig. 11). A first comparison with the measured CT scan shows that the CadMould simulation results sometimes deviate quite significantly and by themselves are not sufficient to meet the reality. Thus, further investigations must follow to identify the reasons for that and to adjust the setup for improving the forecast of fiber orientation.

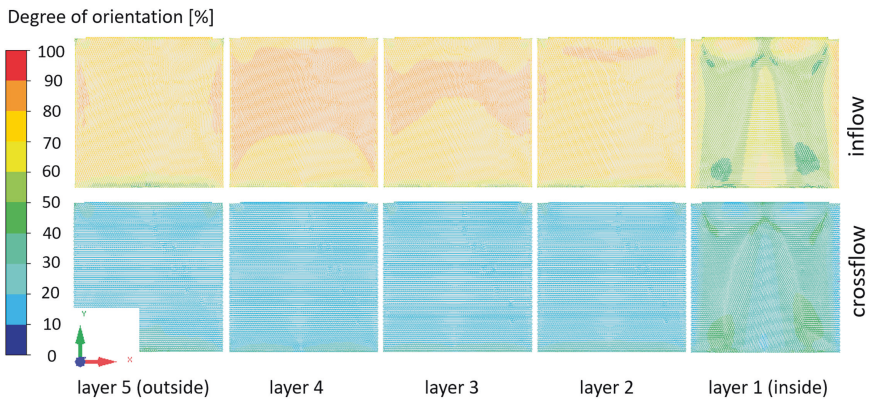


Fig. 10. Fiber orientation per layer

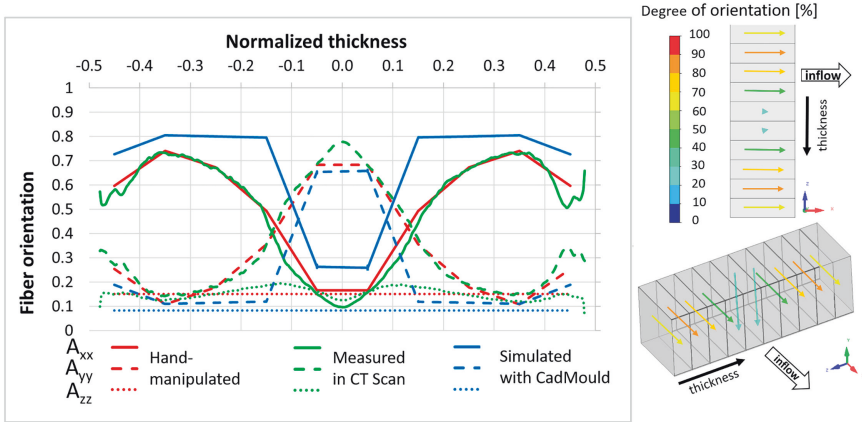


Fig. 11. Fiber orientation across the thickness

3.2 Mapping

For making the fiber orientation output usable for FEA, the exported data need to be converted and transmitted to the FEA mesh. For this, the software tool CONVERSE was used, which provides such an interface between CadMould and Abaqus.

The fiber orientation data were mapped to the final mechanical model. However, the mapped result could not be accepted without further processing due to the deviation in the fiber orientation. Because of the discrepancy in the CadMould simulated results, the mapped output needed to be manipulated, which was done manually by scripting because of less complexity of the sample mesh. The simulation model is still quite manageable in terms of complexity and therefore it was possible with a simple scaling approach to manually edit the fiber orientation definition in the areas to be considered.

Furthermore, the anisotropic/orthotropic material was calibrated based on the sample test results in tension and the measured fiber orientation distribution over the thickness. For this, CONVERSE offers the possibility of carrying out a material calibration based on the tensile test results. Here the material has been adjusted to tension with the appropriate assignment of the fiber orientation via the sample thickness for the first main direction.

3.3 Finite Element Analysis

In a third step the generated files were used for FEA. By means of Abaqus solver the sample geometry was simulated by loading in tension and in compression. The material calibration was done by considering the tensile measurements of test samples and the CT scanning measurements fiber orientation distribution across the thickness. Therefore, the behavior of the sample simulation in loading direction met sufficiently the measured real values taken from DIC (see Fig. 12).

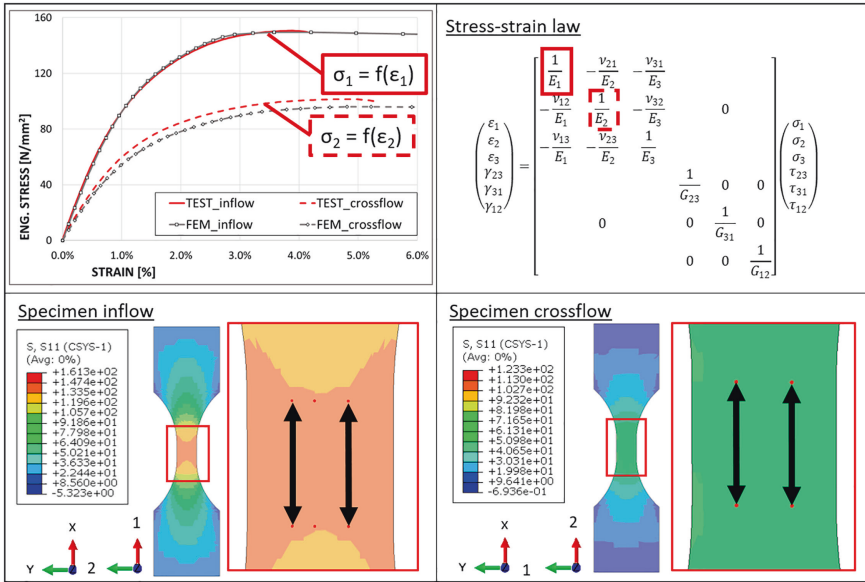


Fig. 12. Tensile behavior of inflow and crossflow samples

3.4 Postprocessing

In post-processing, the technical strain in the different spatial directions and the stress of the virtual sample were evaluated via displacements of the corresponding pairings of nodes. The DIC provides additional technical strain values in second direction perpendicular to loading direction on the sample surface which were compared with the FEA generated results. In the relevant area, the strain values were calculated based on the displacement of node pairs in all the directions and for all the directions as well as the stress is plotted over those strain values. The transverse contraction in-plane is also shown in Fig. 13.

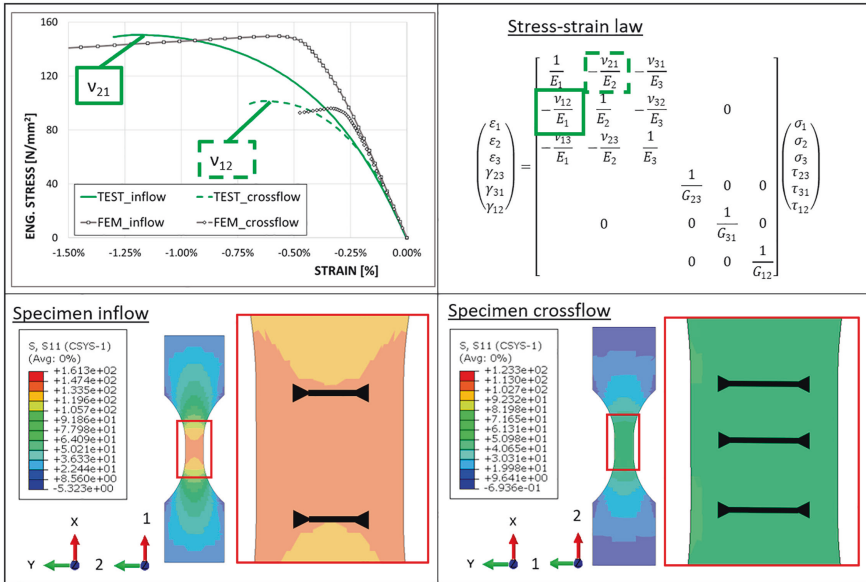


Fig. 13. Transverse contraction in-plane by loading in tension

For the FEM, however, further material data are often missing for a sufficient description of the anisotropic (orthotropic) behavior of a multiphase material like this. However, the DIC opens new ways of recording the transverse contraction in the thickness direction of the sample. This was also compared with the sample behavior in the simulation (see Fig. 14).

The potential of the material is not fully exploited, when loaded in compression. The DIC can also be used to measure strains under compression loads, especially where dimensional limitation does not allow the use of mechanical extensometer. Additionally, buckling effects need to be monitored and imperfection needs to be considered and evaluated. The compression test results of the specimens were compared with the FEM, too (see Fig. 15).

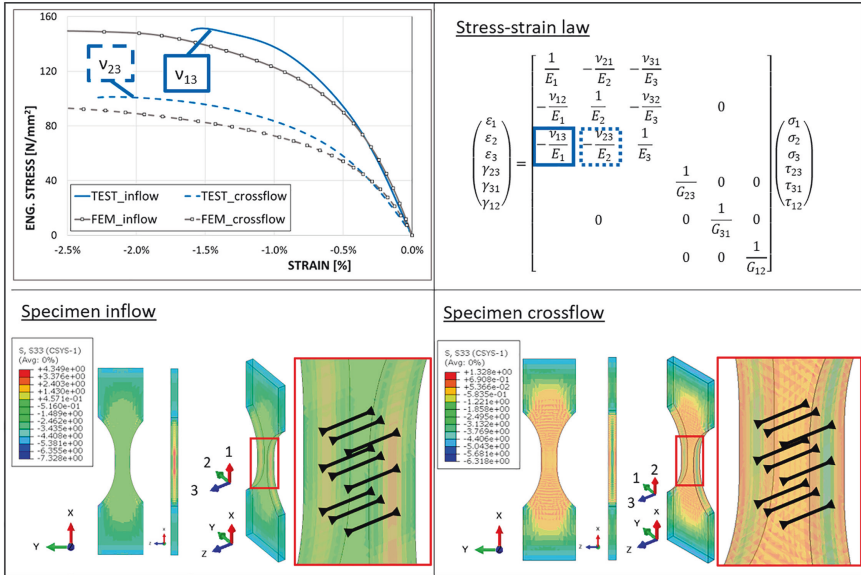


Fig. 14. Transverse contraction out-of-plane by loading in tension

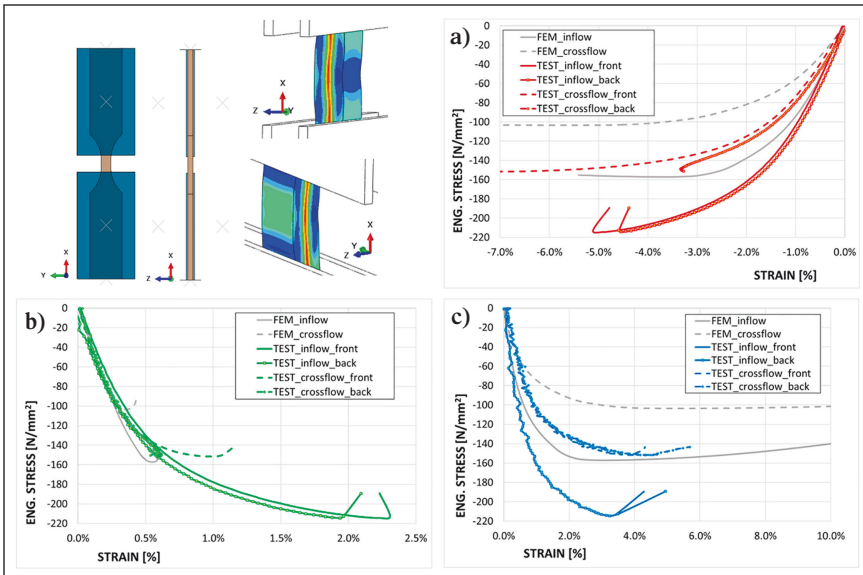


Fig. 15. Compressive behavior of inflow and crossflow samples **a** in loading direction, **b** transverse contraction in-plane and **c** transverse contraction out-of-plane

4 Summary and Outlook

Two materials, unidirectional CFRP and short fiber plastic, were tested in tension and compression in two directions. With the use of digital image correlation, complete stress-strain curves were created with strains in in-plane and out-of-plane direction. For the investigated materials, material properties like Young's modulus and Poisson's ratio were calculated based on these experiments, including transverse contraction in thickness direction.

With numerical methods, the short fiber plastic was simulated, starting from manufacturing process to generate the distribution of fiber orientations. Computer tomographic scans were compared to simulations and used to validate the fiber directions. Adjustments were done to the orientations to have a more correct representation which were then implemented in a material model for FEM. Here, the material behavior in tension and compression loading, including the thickness direction was simulated and compared to experiments.

Complete stress-strain curves, which are necessary for smarter testing using standard test results on coupon level as well as digital twins, can be determined for unidirectional and woven endless fiber reinforced plastics. The substitution of classical strain gauges by digital image correlation allows to measure the third direction Poisson's ratio free of charge, in case of the usage of biplane DIC setup. Additionally, a video is available to investigate the failure mode in more detail.

For short fiber reinforced plastics, material values and allowable cannot be determined directly from standard tests because the fibers have different orientations through the thickness of the specimen. This is similar to element tests for endless fiber reinforced plastics. Based on tension, compression and shear tests, the material values and allowable for a single direction short fiber reinforced material can be determined. According to Fig. 16, the 81 values and allowable needed for a complete 3D characterization of the short fiber reinforced plastic can be determined using results from 320 standard tests at three temperatures and the use of numerical methods in standard software.

A validation – comparison between higher level tests and simulation – will be done in a next step. Infill simulation using different software tools is planned and will be compared to CT-scans. To reduce testing, ALTAIR Multiscale Designer will be used to simulate fiber-matrix behavior on a micromechanical level and will be part of smart testing for the future. Further investigations will be done for the third direction measurements including different materials and the reduction of noise in DIC z-strain measurements.

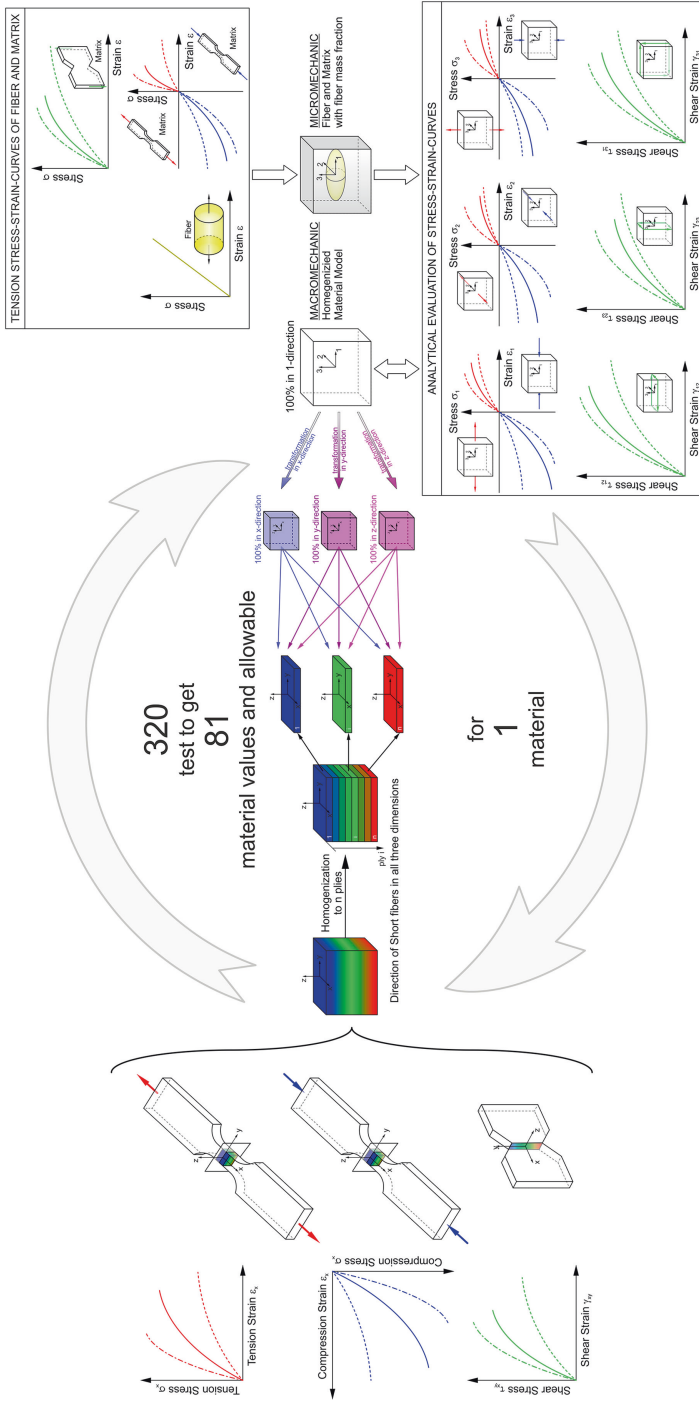


Fig. 16. Complete 3D characterization of short fiber reinforced plastic

Acknowledgement. The research was done in the project RICA (*Reduction of the CO₂-emission by increasing the material utilization using the 3D digital twin*), within the program Technologietransferprogramm Leichtbau (TTP-LB), which is funded by the German Federal Ministry for Economic Affairs and Climate Action. The consortia involved the Universität Der Bundeswehr München, the test house Applus+BKW, the material manufacturers Teijin and Henkel, the aircraft manufacturer Boeing, Altair for numerical simulation methods, Vorwerk Autotec for automotive applications and the small and medium enterprise Eckerle for tooling design and tooling manufacturing.

Supported by:



Federal Ministry
for Economic Affairs
and Climate Action

on the basis of a decision
by the German Bundestag

References

1. Jones, R.M.: Mechanics of composite materials, 2nd edn. CRC Press, Taylor & Francis Group, Boca Raton, London, New York (1999)
2. Schürmann, H.: Konstruieren mit Faser-Kunststoff-Verbunden, 2. Aufl. Springer, Berlin (2007)
3. Korte, N., Bold, J., Höfer, P.: Substitution of Strain Gauges by Optical Strain Measurement for Standard Test Methods of Composite Specimens and Introduction of a New Biaxial Test-Fixture. Proceedings of the Munich Symposium on Lightweight Design **2021**, 13–24 (2022)
4. ASTM International: Test Method for Tensile Properties of Polymer Matrix Composite Materials. ASTM D3039/D3039M-17, West Conshohocken, PA, United States (2017)
5. ASTM International: Standard Test Method for Compressive Properties of Polymer Matrix Composite Materials Using a Combined Loading Compression (CLC) Test Fixture. ASTM D6641/D6641M-16, West Conshohocken, PA, United States (2016)